Author(s): Ostrowska, Malgorzata; Golenya, Irina A.; Haukka, Matti; Fritsky, Igor O.; Gumienna-Kontecka, Elzbieta

Title: Complex formation of copper(II), nickel(II) and zinc(II) with ethyl phosphonohydroxamic acid : solution speciation, synthesis and structural characterization

Year: 2019

Version: Accepted version (Final draft)
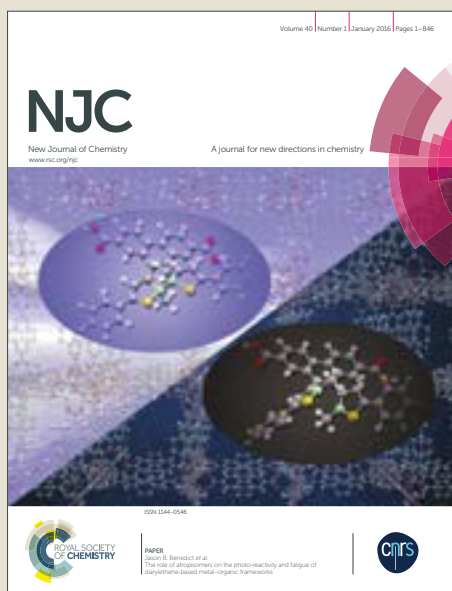
Please cite the original version:

Ostrowska, M., Golenya, I. A., Haukka, M., Fritsky, I. O., & Gumienna-Kontecka, E. (2019). Complex formation of copper(II), nickel(II) and zinc(II) with ethyl phosphonohydroxamic acid : solution speciation, synthesis and structural characterization. New Journal of Chemistry, 26(43), 10237-10249. https://doi.org/10.1039/C9NJ01175G

NJC

Accepted Manuscript

Volume 40 | Number 1 | January 2016 | Pages 1–846

NJC

New Journal of Chemistry
www.rsc.org/njc

A journal for new directions in chemistry

ISSN 1144-0546

ROYAL SOCIETY OF CHEMISTRY

PAPER
Jason B. Benedict et al
The role of atropisomers on the photo-reactivity and fatigue of diarylethene-based metal–organic frameworks

CNरs

This is an Accepted Manuscript, which has been through the Royal Society of Chemistry peer review process and has been accepted for publication.

Accepted Manuscripts are published online shortly after acceptance, before technical editing, formatting and proof reading. Using this free service, authors can make their results available to the community, in citable form, before we publish the edited article. We will replace this Accepted Manuscript with the edited and formatted Advance Article as soon as it is available.

You can find more information about Accepted Manuscripts in the **author guidelines**.

Please note that technical editing may introduce minor changes to the text and/or graphics, which may alter content. The journal's standard **Terms & Conditions** and the ethical guidelines, outlined in our **author and reviewer resource centre**, still apply. In no event shall the Royal Society of Chemistry be held responsible for any errors or omissions in this Accepted Manuscript or any consequences arising from the use of any information it contains.

rsc.li/njc

Complex formation of copper(II), nickel(II) and zinc(II) with ethyl phosphonohydroxamic acid: solution speciation, synthesis and structural characterization

Malgorzata Ostrowska,[a] Irina A. Golenya,[b] Matti Haukka,[c] Igor O. Fritsky,*[b] Elzbieta Gumienna-Kontecka*[a]

[a] Faculty of Chemistry, University of Wroclaw, F. Joliot-Curie 14, 50-383 Wroclaw, Poland; E-mail: elzbieta.gumienna-kontecka@chem.uni.wroc.pl

[b] Department of Chemistry, Taras Shevchenko National University of Kyiv, 64 Volodymyrska Str., 01601 Kiev, Ukraine

[c] Department of Chemistry, University of Jyväskylä, Seminaarinkatu 15 (C building), FI-40100 Jyväskylä, Finland

Abstract

The first example of Cu(II) 12-MC-4 hydroxamic metallacrown containing an ethylphosphonate group as an additional donor function in the β-position with respect to the hydroxamic group, is described. The solution equilibria of ethylphosphonoacetohydroxamic acid (**PAHEt**) with Cu(II) was investigated in aqueous solution by a combination of potentiometry, mass spectrometry, UV-Vis and EPR spectroscopies, and isothermal titration calorimetry. The model containing mononuclear, [CuL], $[CuL_2]^{2-}$ and $[CuL_2H_{-1}]^{3-}$ and pentanuclear, $[Cu_5(LH_{-1})_4]^{2-}$ species is proposed. The predominance of the $[Cu_5(LH_{-1})_4]^{2-}$ species in solution over the pH range 4 - 9 was confirmed by the signals present in ESI-MS spectra, as well as absence of the EPR signal. In addition, the results of isothermal titration calorimetry indicated the stoichiometry of the complex form at pH 5.5 as 1.25. Even if forming less stable MC complex, **PAHEt** offers the formation of 12-MC-4 in a broad pH range, which distinguishes it especially from α-amino hydroxamic acids. The compound corresponding to the pentameric metallacrown complex was isolated in the solid state as {Na_4(H_2O)_6(Ac)[Cu_5(**PAHEt**-3H)_4(Ac)]}_2·3H_2O (**1**), whose crystal structure was determined by X-ray analysis. The centrosymmetric decanuclear complex anion of (**1**) consists of two pentanuclear 12-MC-4 fragments formed by five Cu(II) ions and four triply deprotonated residues of the phosphonohydroxamate ligand, and is associated with eight sodium cations, two acetate anions and twelve water molecules taking part in sodium cations coordination, as well as solvate water molecules. Stability of MCs under conditions of competitive complex formation as well as their reactivity with respect to strong chelating agent, 2,2'-dipyridyl (**dipy**), was examined, and as a result 1D coordination polymer featuring mixed-ligand mononuclear units {[Cu(**dipy**)(**PAHEt**–2H)]}_n·1.86nH_2O (**2**) was formed. In addition the chelating capacity of this ligand toward Ni(II) and Zn(II) ions was studied in solution.

Introduction

Hydroxamate compounds are one of the ligand classes most extensively studied as complexing agents. Their significant high binding affinity to a range of transition metals could be enhanced by the introduction of an additional donor unit.[1, 2] As it was shown, hydroxamate ligands functionalized in α-, β- or γ-position by NH_2- group present peculiar coordination abilities. Their possible (N,N)-(O,O) bridging bis-chelating mode towards Cu(II), Ni(II) and Zn(II) ions results in the formation of metallamacrocycles such as metallacrowns (MCs).[3, 4] MCs are polynuclear complexes that form spontaneously in solution, when a proper conditions, *i.e.* the number of metal ions and ligands, as well as pH, are provided. Taking into account the possible applications of MCs in a number of research fields (in particular, synthesis of porous MOFs for selective absorption of guest molecules, luminescent materials, selective molecular recognition agents)[5-19] over the last two decades their chemistry has largely expanded, revealing that a key aspect in the control of the MCs scaffolds' topology and geometry is a proper match between the metal ion and the ligand.[3, 20-22]

Apart numerous hydroxamate ligands functionalized in α- or β-position by NH_2- group (*e.g.* glycinehydroxamic acid, Glyha, α-alaninehydroxamic acid, α-Alaha, leucinehydroxamic acid, Leuha, β-alaninehydroxamic acid, β-Alaha, Scheme 1), there are only a few examples of hydroxamic acids able to form MCs while having donor groups other than the amino group, and these include picolinehydroxamic acid, Picha, quinaldinehydroxamic acid, Quinha, salicylhydroxamic acid, Shi, and malonomonohydroxamic acid, MACZ (Scheme 1). Ligands with salicyl and carboxylate donors are of special interest as they provide additional negative charge thus making the MC moiety anionic; they can also supply (like in the case of carboxylic groups) additional donor and/or bridging functions, which together with the overall negative charge of the species, is a strong prerequisite for exo-coordination of additional metal ions in the plane of MC scaffold. In its turn, this would result in the formation of extended polynuclear assemblies of higher nuclearity with MC core. Unlike numerous MC-based assemblies obtained with the use of axial binding of MC moieties, in particular, 1-, 2- and 3D-coordination polymers, including porous MOFs,[23-25] the possibility to obtain of discrete exchange clusters or layered assemblies through of in-plane exo-coordination to MC is still poorly explored. Such systems could be of interest because of their original magnetic, spectral or luminescent properties. To date only one analogue, malonomonohydroxamic acid (MACZ), was investigated in solution to monitor its speciation and ability to form MCs.[26] It was shown that the use of easily deprotonated carboxylate as the peripheral donor group allowed to enlarge the pH range of MC's self-assembly (in comparison to aminohydroxamates).[26]

α -functionalized hydroxamic acids

| Glyha | α-Alaha | Leuha | Picha | Quinha |

β-functionalized hydroxamic acids

| β-Alaha | Shi | MACZ |
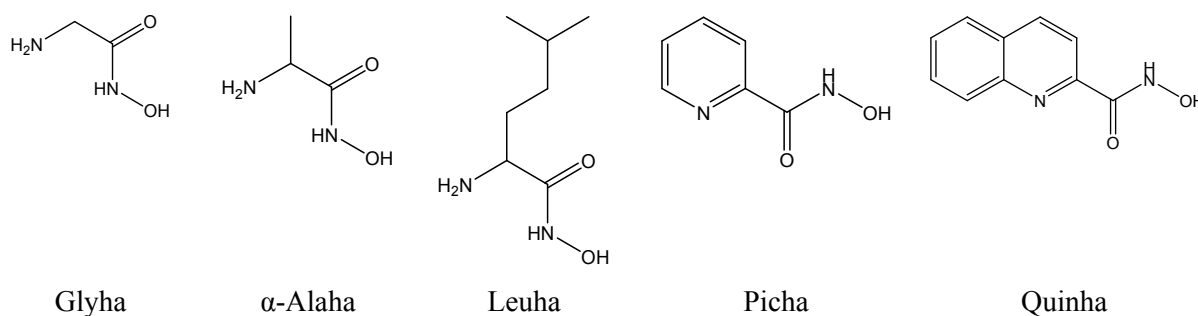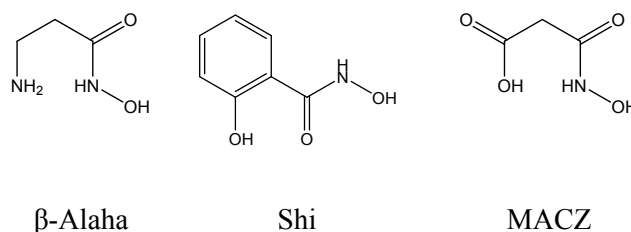
Scheme 1. Representation of α- and β-functionalized hydroxamic acids forming MC species. Abbreviations used: Glyha = glycinehydroxamic acid, α-Alaha = α-alaninehydroxamic acid, Leuha = leucinehydroxamic acid, Picha = picolinehydroxamic acid, Quinha = quinolinehydroxamic acid, β-Alaha = β-alaninehydroxamic acid, Shi = salicylhydroxamic acid, MACZ = malonomonohydroxamic acid.

Inspired by these results, we decided to modify the structure of MACZ ligand by the substitution of the β-carboxylate group for ethyl phosphonate unit, and here we report Cu(II) 12-MC-4 complex of ethylphosphonoacetohydroxamic acid (**PAHEt**), both its formation in solution and detailed structural characterization in solid state. The specific complexing properties of phosphonate groups are well known and documented.[27, 28] Although the binding ability of simple monophosphonate ligands is not very strong, its combination with an additional, strongly coordinating donor, such as amino nitrogen or thioether sulphur in one molecule was shown to significantly improve the metal chelation capability of these ligands. For example, the stability constants of aminophosphonate complexes with metal ions are higher than those of simple phosphonates or amino acids.[27, 28] Similarly to the carboxylic group, the phosphonate function can bind metal ions through various binding modes, including several bridging possibilities, and this enhanced potential of structural diversification is especially revealed in biologically active compounds.[28] Generally, the phosphonate complexes of 3d-transition metal ions are less stable than the carboxylate complexes of analogous structure, however, unlike the carboxylic group, the phosphonate group is not planar and provides an additional negative charge what may result in a better water solubility of MCs (important for biomedical applications) and more versatile exo-coordination of the metal ions to the MC scaffold (*e.g.* not pure in-plane exo-

coordination and binding of metal ions with higher positive charge). Therefore, one can expect that the combination of the two, specific phosphonate and strong hydroxamate, donor groups in one ligand molecule can result not only in the formation of MCs with vacant exo-binding sites but also in the realization of alternative coordination modes and metal chelating patterns. In its turn, this could give rise to polynuclear assemblies and MOFs with specific versatile topologies.

PAHEt is a derivative of a phosphonoacetohydroxamic acid (PAH) which is known to be an efficient inhibitor of enolase (EC 4.2.1.11).[29] Interestingly, the binding mode of PAH in the inhibited enzyme is different than the one typical for hydroxamates, *i.e.* through (O,O')-chelation (Scheme 2a). In the inhibited enolase, PAH is bound in a bis(chelate) mode, coordinating two zinc ions with the formation of a six-membered ring (O_{posph}, $O'_{carbonyl}$) and a five-membered ring ($O'_{carbonyl}$, $O''_{hydroximate}$), with common carbonyl oxygen atom playing a bridging function (Scheme 2b). As the described binding motif is not present in MC complex (Scheme 2c, *vide infra*), this demonstrates a versatility of the coordination possibilities of phosphono-hydroxamate compounds.
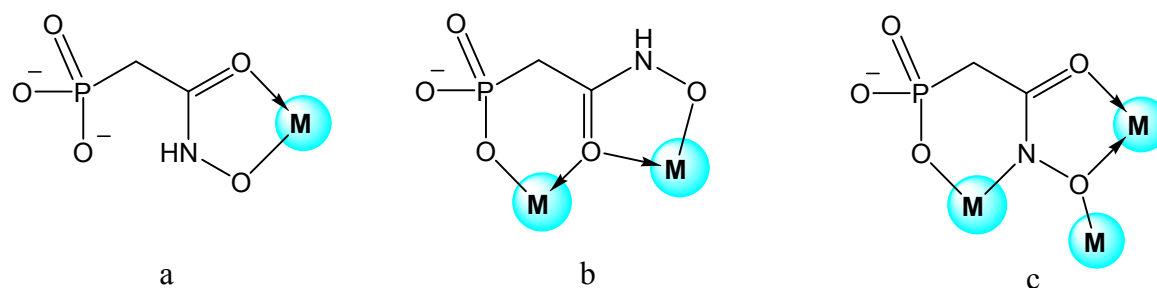
Scheme 2. The possible binding modes of **PAH** in the inhibited enolase (a, b) and in MC (c).

Experimental

Reagents

All of the chemicals used in this work were of analytical grade and used without further purification. Triethyl phosphonoacetate was purchased from Fluka. Solutions of NaOH, HCl, NaCl, $ZnCl_2$, $NiCl_2$ and $CuCl_2$ were prepared from pure commercial products (Sigma Aldrich or POCH). Cu(II), Ni(II) and Zn(II) stock solutions were standardized by ICP-AES along with the complexometric titration with standardised Na_2H_2EDTA and murexide ($CuCl_2$ and $NiCl_2$) and xylenol orange ($ZnCl_2$). HCl solution was titrated by standardized NaOH solution. Carbonate-free NaOH solution was standardized by titration with potassium hydrogen phthalate (POCH).

Syntheses and crystallization

Disodiummethylphosphonoacetohydroxamate {Na$_2$(PAHEt-2H)}. To the mixture of solution of triethylphosphonoacetate (4 ml, 20 mmol) in water (20 ml) and solution of hydroxylammonium chloride (1.7 g, 24 mmol) in water (20 ml), solution of sodium hydroxide (4N, 10 ml) was added drop wise on continuous stirring. The obtained mixture (pH ≈ 12) turned yellowish, and stirring has been continued for 24 h at ambient temperature. Then the volume of the solution was reduced on a rotary

evaporator, and iso-propanol (100 ml) was added to the residue. The formed precipitate was filtered

washed with iso-propanol and dried. The crude product was recrystallized from hot water as colorless

fine crystals. Yield 3 g (66 %).ESI-MS m/z 227.3; ^{1}H NMR (DMSO-d^6, 400 MHz): δ3.70 (2H, dq,

CH$_2$), 2.51 (2H, d, CH$_2$), 1.1 (3H, t, CH$_3$); ^{31}P NMR (DMSO-d^6, 400 MHz): δ16.5; FTIR (cm^{-1}): 3300

ν$_{N-H}$, 1620 ν$_{C=O}$, Amide I, 1250 ν$_{P=O}$, 1090, 970 ν$_{N-O}$, 855ν$_{P-O}$.

{Na$_4$(H$_2$O)$_6$(Ac)[Cu$_5$(PAHEt-3H)$_4$(Ac)]}$_2$·3H$_2$O   (1). Aqueous   solution   of

Cu(CH$_3$COO)$_2$·H$_2$O (0.1 M, 0.5 mmol, 5 ml) was added to solution of {Na$_2$(**PAHEt**-2H)} in methanol

(0.1 M, 0.4 mmol,4 ml), then the resulting solution was filtered and set for evaporation in the air at

room temperature until dark-green precipitate was formed. The obtained precipitate was dissolved in

methanol, and the solution was subjected to slow diffusion of vapors of methyl tert-buthyl ether. After

72 h, dark-green crystals were obtained; they were filtered, washed with methyl tert-buthyl ether and

air-dried. Yield69 %. Elemental analysis for C$_{40}$H$_{98}$Cu$_{10}$N$_8$Na$_8$O$_{63}$P$_8$(2766.39) calc. (%): C, 17.37; H,

3.57; N, 4.05; Cu, 22.97;found, (%): C, 17.55; H, 3.69; N, 3.76; Cu, 23.11.FTIR (cm^{-1}): 1590 ν$_{C=O}$,

Amide I, 1260 ν$_{P=O}$, 1040, 930 ν$_{N-O}$.

{[Cu(dipy)(PAHEt–2H)]}$_n$·1.86nH$_2$O (2). Solution of Cu(ClO$_4$)$_2$·6H$_2$O (0.1 M, 0.25 mmol,

2.5 ml) in methanol was added to solution of {Na$_2$(**PAHEt**-2H)} in methanol (0.1 M, 0.2mmol, 2 ml),

then solution of 2,2'-bipyridyl in methanol (1 M, 0.2 mmol, 0.2 ml) was added to the obtained

mixture. The resulting dark-green solution was filtered, and the filtrate was set aside for evaporation in

the air at room temperature. Dark-green crystals formed within 36 h were filtered, washed with cold

water and air-dried. Yield 88%. Elemental analysis for C$_{14}$H$_{19.72}$CuN$_3$O$_{6.86}$P (434.32) calc. (%): C,

38.72; H, 4.58; N, 9.67; Cu, 14.63; found, (%): C, 38.28; H, 4.69; N, 9.81; Cu, 14.32. FTIR (cm^{-1}):

3300 ν$_{N-H}$, 1590 ν$_{C=O}$, Amide I, 1260 ν$_{P=O}$, 1040, 930 ν$_{N-O}$.

X-Ray analysis

Measurements were carried out on a Bruker SMART APEX II CCD diffractometer at 293(2)

K with horizontally mounted graphite crystal as a monochromator and Mo-K$_α$ radiation (λ = 0.71073

Å). Data was collected and processed using *APEX 2*.[30] A semi-empirical absorption correction

(*SADABS*) [31] was applied to all data. The structures were solved by direct methods (*SHELXS-97*)[32] and

refined by full-matrix least-squares on all F_o^2 (*SHELXL-2014/7*)[33] anisotropically for all non-hydrogen

atoms.

(1): The methylene carbon atom C3 and water oxygen atom O32 appeared to be disordered over two

positions, the occupancy factors were found to be equal 0.729/0.271 and 0.35/0.15, respectively. The

water hydrogen atoms were either located from the difference Fourier map or located by using

HYDROGEN program.[34] All O-H hydrogen atoms were constrained to ride on their parent atom, with

U$_{iso}$ = 1.5U$_{eq}$ (parent atom). Other hydrogen atoms were positioned geometrically and were also

constrained to ride on their parent atoms, with C-H = 0.95-0.99 Å, and U$_{iso}$ = 1.2-1.5 U$_{eq}$ (parent atom).

(2): The methyl carbon atom C14 appeared to be disordered over two positions with occupancies 0.86/0.14. The water oxygen atom O6 was found to have an occupancy factor 0.86. The O-H hydrogen atoms were located from the difference Fourier map but constrained to ride on their parent atom, with $U_{iso} = 1.5U_{eq}$(parent atom). Other hydrogen atoms were positioned geometrically and were also constrained to ride on their parent atoms, with C-H = 0.95-0.99 Å, and $U_{iso} = 1.2$-1.5 U_{eq} (parent atom).

Solution studies

The potentiometric titrations were performed at a constant temperature of 25°C in an atmosphere of argon as an inert gas, using an automatic titrator system Titrando 905 (Methrom), connected to a combined glass electrode (Mettler Toledo InLab Semi-Micro) calibrated daily for hydrogen ion concentration using HCl. All the titrations were performed on 0.1M solutions, using NaCl as a background electrolyte. Starting volumes of *ca.* 3mM ligand solutions were 3ml, and the exact concentration of the ligand was determined using the method of Gran.[35] Metal-to-ligand molar ratios were 1:2 and 1:3 for all metal ions. The potentiometric data, collected over a pH range 2.0-11.0, were refined with the SUPERQUAD[36] program, which use nonlinear least-squares methods. The species distribution diagrams were generated using a computer HYSS program.[37]

Electrospray ionization mass spectrometry (ESI-MS) data were recorded on a BrukerQ-FTMS spectrometer. The instrumental parameters were: scan range, m/z 200−1600; dry gas, nitrogen; temperature, 170 °C; capillary voltage, 4500 V; ion energy, 5 eV. The capillary voltage was optimized to the highest signal-to-noise ratio. The spectra were recorded in the negative ion mode. MeOH/H_2O solvent (50/50 v/v) was used to prepare solutions of ligand with concentrations of 10^{-4} to 10^{-5} M and metal-to-ligand molar ratios 1:1, 1:2 and 1:3.

The absorption spectra were recorded on a Varian Cary 300 Bio and Varian Cary 50 UV-Vis spectrophotometers using a Hellma quartz optical cells with 1 cm and 5 cm path length for Cu(II) and Ni(II) complexes respectively. Sample solutions had compositions similar to those employed in the potentiometry and the metal ions concentrations were 1mM for Cu(II) and 3mM for Ni(II). The initial pH of solutions was adjusted to around 2 and then the titration of the solution was carried out by the addition of small volumes of NaOH. Data were processed using Origin 7.0.

Electron paramagnetic resonance spectra were recorded on a Bruker ELEXSYS E500 CW-EPR spectrometer equipped with an NMR teslameter (ER 036TM) and frequency counter (E 41 FC) at X-band frequency, at 77 K. The metal concentration was 1mM, and the metal-to-ligand ratio was 1:3. The solutions for EPR were prepared with addition of 30% of ethylene glycol as a cryoprotectant. The spectra were recorded in the pH range from 2.50 to 11.00. The pH of samples was adjusted to expected by use of appropriate volumes of HCl and NaOH solutions. The experimental spectra were simulated using WINEPR Simfonia 1.26 program and Spin (EPR OF S>1/2) program by Dr. Andrew Ozarowski, National High Field Magnetic Laboratory, University of Florida.

ITC measurements

ITC experiments were performed using a Nano ITC calorimeter (TA Instruments) with a cell of standard volume of 1.0 ml (24K gold).To the 2 mM **PAHEt** in 20 mM sodium acetate aqueous solution, aliquots of the 8 mM $CuCl_2$ in 20mM sodium acetate aqueous solution were added using 250 μl syringe; the stoichiometry from 0 to 1.6 Cu(II) to ligand was thus obtained. The pH of both solutions was 5.5. The total number of 40 injections,6 μl each were added after the calorimeter finalized the primary equilibration, with 300 s apart. The solution in the cell was stirred by the syringe at 250 rpm. The calorimeter was operated using the Nano ITC Run software v. 2.2.3, and all the data obtained were analysed with the NanoAnalyze v. 2.4.1 program. The independent model was used to evaluate the results obtained and the control experiments were performed in each case; the enthalpies of reagents dilution were subtracted from the enthalpies of supramolecular binding processes.

Results and discussion

Protonation and complex formation equilibria in aqueous solution

To evaluate the coordination properties of ethylphosphonoacetohydroxamic acid (**PAHEt**, H_2L) towards Cu(II), Ni(II) and Zn(II) in solution, first the acid-base properties of the ligand were determined. **PAHEt** possesses one ethylphosphonic group and one hydroxamic unit. In the measured pH range, *i.e.* 2-11, the ligand was observed to release only one proton, and therefore it is treated as $[HL]^-$. The calculated $pK_a = 9.54$ corresponds to the ionization of hydroxamic unit and it is in good agreement with the literature data obtained for similar systems.[1, 22, 26] The phosphonic proton dissociation occurs much below pH 2 and the constant corresponding to this process could not be determined under our experimental conditions.[38-40]

The potentiometric studies of Cu(II)/**PAHEt** system revealed the formation of mono- and polynuclear complexes. The best fitting of the experimental and calculated potentiometric curves were obtained for the model containing four complexes: $[CuL]$, $[Cu_5(LH_{-1})_4]^{2-}$, $[CuL_2]^{2-}$ and $[CuL_2H_{-1}]^{3-}$ (Table 1, Fig. 1). According to the model, the complexation starts below pH 2 with the $[CuL]$ species. Slightly above pH 3, the formation of the 12-MC-4 complex $[Cu_5(LH_{-1})_4]^{2-}$ is proposed, with the species predominating the solution in the pH range from 4 to ~9, reaching 90% of total Cu(II) at pH *ca.*5. At pH above 9, the $[CuL_2]^{2-}$ and $[CuL_2H_{-1}]^{3-}$ species are present in solution.
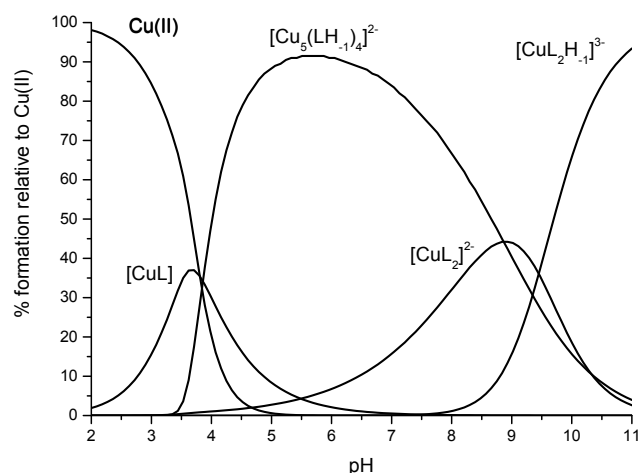
Fig. 1. Species distribution diagram for the Cu(II)-**PAHEt** system. Cu(II):L = 1:3, [L] = 3mM, I = 0.1 M NaCl, 25° C.

In order to confirm the proposed model, first we have carried out ESI-MS experiments, with the spectra recorded for 1:1, 1:2 and 1:3 metal-to-ligand ratios at pH 3.0 and 8.0. In all spectra, only the anionic species corresponding to Cu(II) 12-MC-4 complex were detected, *i.e.* $[Cu_5(LH_{-1})_4]^{2-}$, m/z = 518.34, and $\{(Na^+)[Cu_5(LH_{-1})_4]\}^-$, m/z = 1059.66, (Figure 2). A comparison between experimental and simulated isotopic patterns of the negatively-charged complex showed an excellent agreement (Figure 2). However, the absence of the signals of mononuclear species is not proof of the absence of complexes in solution. It has to be underlined, that [CuL] species is neutral and may not be easily ionized in ESI-MS experiment, while an expected m/z of $[CuL_2]^{2-}$ is 212.79, and the scan range of the ESI-MS equipment started from m/z 200, so it is almost impossible to detect ions with such a low m/z.
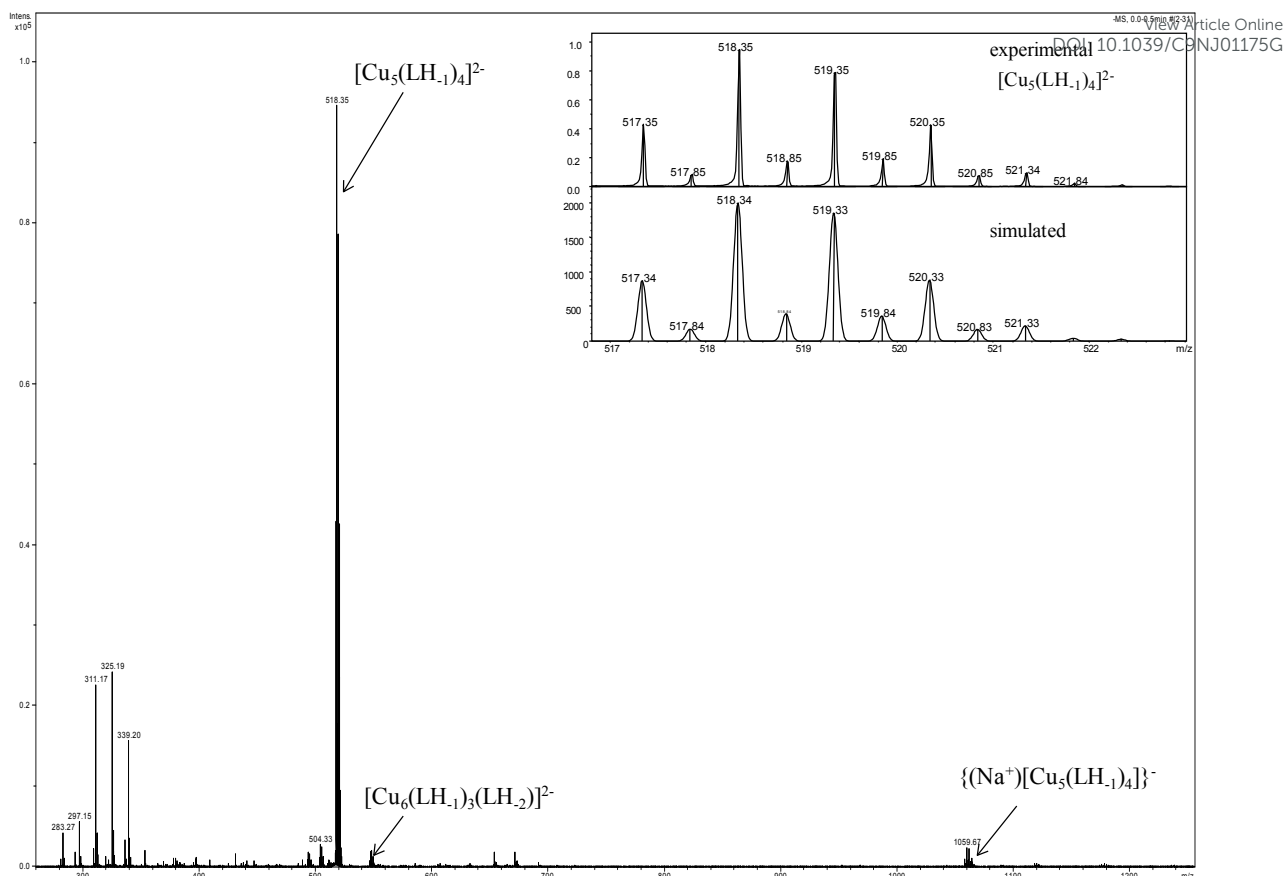
Fig. 2. ESI-MS spectra of Cu(II)/**PAHEt** system, metal-to-ligand ratio of 1:1 at pH 8, and the comparison between experimental and simulated isotopic patterns of the complex $[Cu_5(LH_{-1})_4]^{2-}$.

To further characterize the complex species formed between Cu(II) and **PAHEt**, UV-Vis and EPR experiments were carried out. Below pH 2.5, a UV-Vis absorption spectra exhibit a transition around 800 nm assigned to the d-d band of free $Cu(II)_{aq}$ ion (Figure S1). At pH ~3, the spectra are characterized by a d-d band with maximum at ca. 720 nm ($\varepsilon = 26$ $M^{-1}cm^{-1}$) indicating one nitrogen donor beside oxygen atom involved in Cu(II) coordination, and a ligand-to-metal charge-transfer transition, LMCT, at 320 nm ($\varepsilon = 227$ $M^{-1}cm^{-1}$), previously attributed to N^--$O^-_{(nitrogen)} \rightarrow Cu(II)$ and N^--$O^-_{(oxygen)} \rightarrow Cu(II)$ CT transitions, [41, 42] (Table 1, Figure S1). The parameters of corresponding EPR spectra ($A_{II} = 149$ G and $g_{II} = 2.34$) (Table 1, Fig. 2) support the formation of the complex with the {O, N} mode of binding; all together, the spectral characteristics can be ascribed to the formation of [CuL] species. With an increase of pH, the maximum of d-d band moves to 675 nm ($\varepsilon = 415$ $M^{-1}cm^{-1}$). The EPR spectra recorded at 77K in the pH range 5-8 are silent (Fig. 3), which strongly supports the model without the presence of any mononuclear Cu(II) complexes which are expected to be EPR active. A silencing of the EPR signal is typical for polynuclear Cu(II) species, and was earlier observed for the majority of Cu(II) 12-MC-4 complexes;[1, 22, 25, 26] to date only two 12-MC-4 were revealed not EPR-silent, but both measured at 4–6 K.[43, 44]   According to the potentiometric calculations, the species dominating in solution from pH 4 to 9 is $[Cu_5(LH_{-1})_4]^{2-}$, and the EPR

behaviour is consistent with this finding. The formation of $[CuL_2]^{2-}$ and $[CuL_2H_{-1}]^{3-}$ species is accompanied by slight blue-shift of the d-d bands (to 670 nm) and reappearance of the EPR spectrum; an increase of A_{II} and a decrease of g_{II} (Table 1, Fig. 3) point to the coordination of an additional nitrogen atom to Cu(II) ion. The proposed structures of $[CuL]$, $[Cu_5(LH_{-1})_4]^{2-}$, $[CuL_2]^{2-}$ and $[CuL_2H_{-1}]^{3-}$ are depicted in Scheme 3.
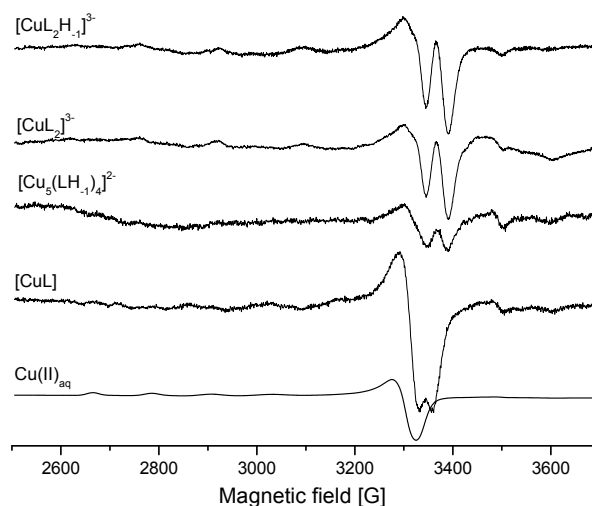

Fig. 3. EPR spectra of Cu(II) complexes with **PAHEt** ligand. Metal-to-ligand molar ratio of 1:3, $[L] = 3mM$.

Table 1 Complex formation constants and spectroscopic parameters of Cu(II), Ni(II) and Zn(II) complexes with **PAHEt** in aqueous solution[a]

Species	Potentiometry	UV-Vis		EPR	
	$\log\beta$	λ_{max} [nm]	ε [mol^{-1}dm^{3}cm^{-1}]	A_{II} [G]	g_{II}
Cu(II) complexes					
[CuL]	8.35(2)	720	26	149	2.34
		320	227		
$[Cu_5(LH_{-1})_4]^{2-}$	31.18(3)	675	415	[b]	[b]
		320	4.9×10^3		
$[CuL_2]^{2-}$	15.07(4)	670	78	167	2.29
		320	1×10^3		
$[CuL_2H_{-1}]^{3-}$	5.62(3)	670	78	167	2.29
		320	1×10^3		
Ni(II) complexes					
[NiL]	5.73(2)	660	4		
		400	12		
$[NiL_2]^{2-}$	9.74(3)	660	6		
		400	20		

$[NiL_2H_{-1}]^{3-}$	-1.12(3)	660	7
		400	22
$[NiL_2H_{-2}]^{4-}$	-12.35(2)	660	7
		400	22

Zn(II) complexes

$[ZnL]$	4.83(3)
$[ZnL_2]^{2-}$	8.55(6)
$[ZnL_2H_{-1}]^{3-}$	-1.44(6)
$[ZnL_2H_{-2}]^{4-}$	-12.06(8)

[a] I = 0.1M (NaCl), T = (25.0 ± 0.2) ˚C. The reported errors on log β are given as 1σ and experimental errors on λ_{max} = ±2nm. [b] EPR silent.
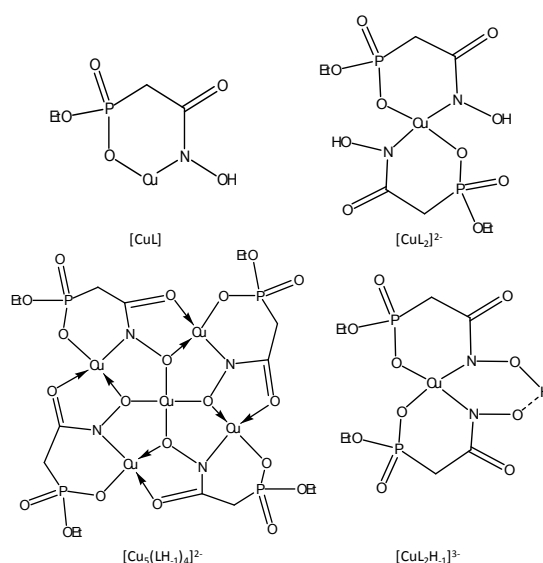
Scheme 3 Schematic representation of the proposed structures of [CuL], $[Cu_5(LH_{-1})_4]^{2-}$, $[CuL_2]^{2-}$ and $[CuL_2H_{-1}]^{3-}$ complexes.

For the Ni(II) and Zn(II)/**PAHEt** systems, only the formation of mononuclear complexes was observed. Calculations based on the potentiometric titrations suggest the formation of four species: $[ML]$, $[ML_2]^{2-}$, $[ML_2H_{-1}]^{3-}$, $[ML_2H_{-2}]^{4-}$ for both metal ions (Table 2, Fig. 4). The UV-Vis spectroscopic characteristics, with the d–d transitions centred at 400 and 660 nm present in the entire range of pH (Table 3, Fig. S2), suggest an octahedral coordination of the Ni(II) ions. The recorded ESI-MS spectra indicate only the formation of mononuclear complexes with the metal-to-ligand molar ratio 1:1, $\{[NiL](Cl)\}^-$ (*m/z* = 273.92) and $\{[ZnL](Cl)\}^-$ (*m/z* = 279.91) (Fig. S3).
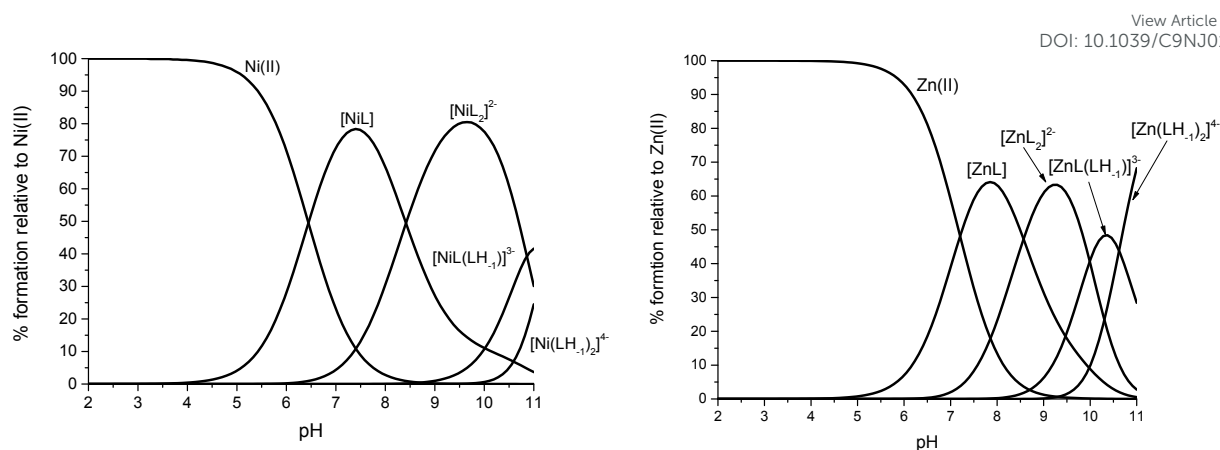
Fig. 4. Species distribution diagram for the Ni(II)-**PAHEt** and Zn(II)- **PAHEt** systems. Metal-to-ligand ratio of 1:3, [L] = 3mM, I = 0.1 M NaCl, 25° C.

The stability of the MC species formed by **PAHEt** is comparable to that reported for MACZ ligand[26] (Table 2), in which a carboxylate group was introduced in the β-position with respect to the hydroxamic function. This modification resulted in the formation of a 12-MC-4 complex in a broad pH range (4-11).[26] The replacement of the carboxylate group for the ethylphosphonate analogue, created the ligand with a similar behaviour. The $[Cu_5(LH_{-1})_4]^{2-}$MC complex predominates in solution in pH 4-9. A comparison of the stability constants of the two MC complexes, reveals however a 2.75 log units lower stability of the latter, **PAHEt** ligand (Table 2). This behaviour is certainly due to higher acidity of ethylphosphonate function in comparison to the carboxylate group. As expected, even higher decrease in stability is observed in relation to β-aminohydroxamate ligands, like β-Alaha, or α-derivatized hydroxamic acids, as Glyha, α-Alaha, or Picha (Scheme 1), possessing more effective amino or pyridine nitrogen donors (Table 2). Of importance, even if less effective, **PAHEt** offers the formation of 12-MC-4 in a broad pH range, which distinguishes it especially from α-amino derivatives, and might be an important feature if one thinks about analytical applications of MCs.

Unfortunately, the formation of the Ni(II) and Zn(II) MCs of **PAHEt** ligand was not observed, most probably due to their lower stability in comparison to Cu(II) complexes (Table 1). It is rather typical behaviour due to the different nature of the metal ions, being in line with the Irving-Williams series. For [ML], $[ML_2]^{2-}$ and $[ML_2H_{-1}]^{3-}$, species formed by all three metals, Cu(II) complexes are 3-7 log units more stable than the corresponding Ni(II) species, while logβ of [NiL] and $[NiL_2]^{2-}$ complexes are *ca.* one log unit greater than those of Zn(II) species (Table 1).

Table 2 Logarithms of complex formation constants for 12-MC-4 complexes of Cu(II) and various hydroxamic acids.[a]

Ligand	log β	I	Reference
PAHEt	31.18	0.1M (NaCl)	This work
MACZ	33.93	0.1M (KNO$_3$)	[26]
Glyha	39.96	0.1M (KCl)	[45]
α-Alaha	40.03	0.1M (KCl)	[46]
Leuha	39.44	0.1M (KCl)	[45]
Picha	38.65	0.1M (KCl)	[20]
β-Alaha	49.39	0.1M (KCl)	[46]

[a]Abbreviations used: Glyha = glycinehydroxamic acid, α-Alaha = α-alaninehydroxamic acid, Leuha = leucinehydroxamic acid, Picha = picolinehydroxamic acid, β-Alaha = β-alaninehydroxamic acid

Isothermal titration calorimetry

The ITC method is a useful tool for the investigation of the metal-ligand interactions in solution and can be used as an additional techniques to prove the stoichiometry of the complex formed in solution. ITC measurements of Cu(II) binding to **PAHEt** ligand at pH 5.5 have been performed in order to confirm the stoichiometry of the complex dominant in the solution at this pH. The approximation curves of the experimental data and their thermodynamic characteristics are presented in Fig. 5. The inflection point in the titration curve, showing the enthalpy *vs.* metal-to-ligand molar ratio, clearly indicates that the stoichiometry of the complex formed at pH 5.5 is 1.25, which may correspond to five metal ions coordinated by four **PAHEt** ligands. This result strongly supports our potentiometric calculations, and confirm the presence of $[Cu_5(LH_{-1})_4]^{2-}$ complex in a significant amount at pH 5.5. A series of systematic calorimetric studies on Cu(II) 12-MC-4 complexes with α-, β, or γ- hydroxamate ligands were reported earlier. [45, 47, 48] It was shown that both enthalpic and entropic terms are favourable to the pentameric species formation, although the entropic contributions are always higher, than the enthalpic terms, which are negative in all reported cases.[45, 47, 48] However, the ΔH value of Cu(II)-**PAHEt** 12-MC-4 formation is positive indicating that the process is endothermic. It should be mentioned, that the overall energetic effect of the complexation consists of the dehydratation of the metal cation and the ligand, $\Delta H_{dehyd}>0$, the formation of new metal-ligand bonds $\Delta H_{bind}<0$, as well as dissociation of the metal ion from the buffer. [49-51] Taking into account all of those factors, the thermodynamic parameters obtained for the studied system revealed that the formation of the complexes is an entropy-driven process ($|\Delta H|<|T\Delta S|$). The positive value of the enthalpy change of the complexation reaction, ΔH, indicate that the positive endothermic effect due to the dehydratation of the Cu(II) ions and the positive endothermic effects caused by the dissociation of the Cu(II) ion from acetate buffer is not overcompensated by an exothermic effect associated with the formation of new metal-ligand bonds.

Summarizing, the comparison of thermodynamic parameters obtained here for Cu(II)-**PAHEt** MC, and those reported earlier for other MCs should be done carefully since, as it was mentioned above, the interactions between the metal ions and ligands strongly depend on specific conditions

used, *i.e.* pH, protonation stage, interaction with the buffer etc. Despite the non-identical conditions the data stay in good agreement. Moreover, to relate the stability of 12-MC-4 complex obtained from potentiometric and ITC data, we have used Hyss program to calculate an apparent stability constant at pH = 5.5, including stability constants determined by potentiometry (Table 1) and concentration ranges used in ITC ($c_{Cu(II)}$ from 0.048 up to 1.6 mM, c_{PAHEt} = 1.6 mM). The estimated $\log K_{app}$ = 4.77 is in perfect agreement with $\log K_{ITC}$ = 5.11.

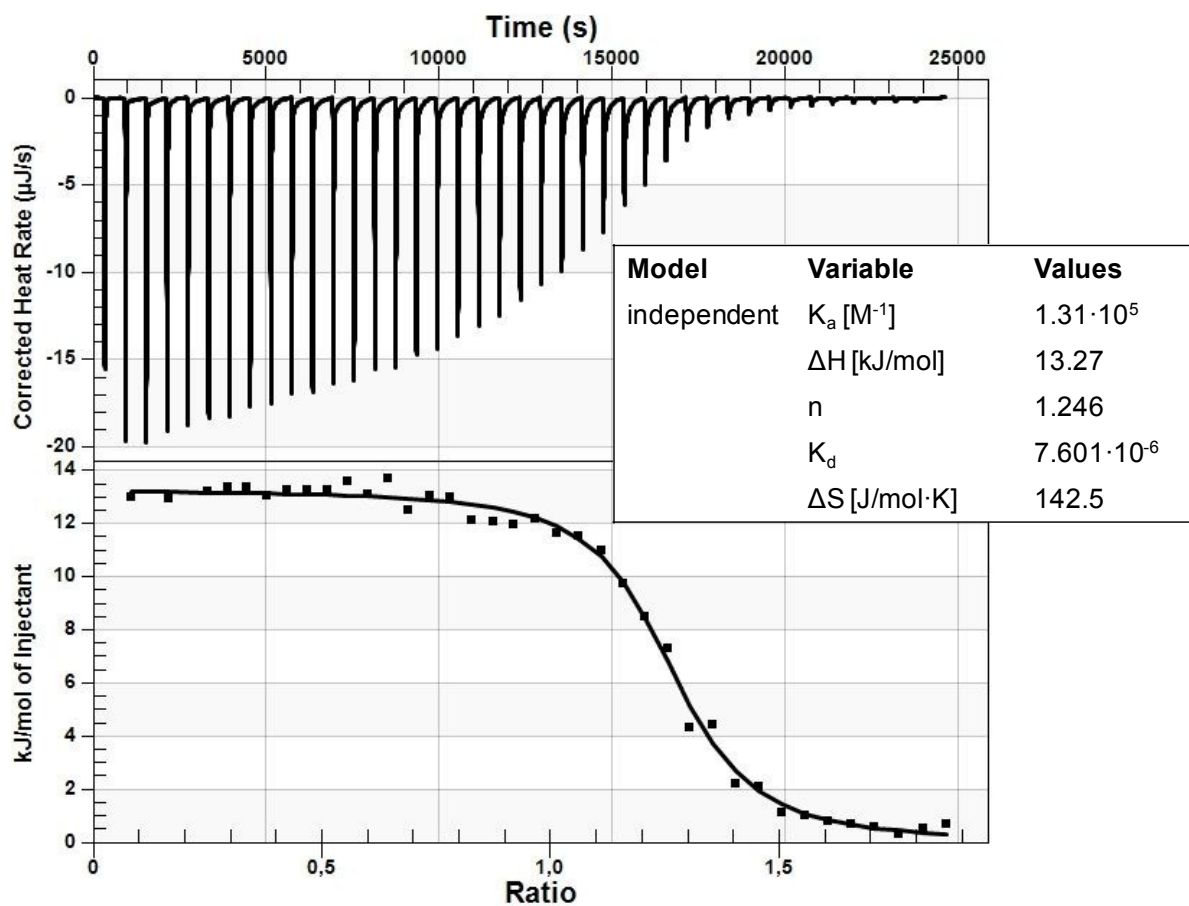| Model	Variable	Values
independent	K_a [M^{-1}]	$1.31 \cdot 10^5$
	ΔH [kJ/mol]	13.27
	n	1.246
	K_d	$7.601 \cdot 10^{-6}$
	ΔS [J/mol·K]	142.5

Fig. 5. ITC experiment of the titration of Cu(II) into **PAHEt** ligand (top) and experimental data (points) and their approximation curves (line) (bottom).

Synthesis and molecular structure of coordination compounds

As according to the results of speciation study the pentanuclear 12-MC-4 species is dominating the solution in the pH range 4 – 9, the synthetic attempts aiming in isolation of corresponding coordination compounds were carried out in aqueous or mixed solvents solutions under appropriate conditions, using 5:4 or 1:1 metal-to-ligand stoichiometry and different starting Cu(II) salts and alkaline agents. When Cu(II) acetate was used, a green precipitate was obtained, that when redissolved in methanol, and subjected to slow diffusion of methyl tert-butyl ether, formed single crystals of complex **{Na$_4$(H$_2$O)$_6$(Ac)[Cu$_5$(PAHEt-3H)$_4$(Ac)]}$_2$·3H$_2$O (1)**. The elemental analysis,

together with IR spectroscopic characteristics of (**1**) suggested the formation of metal-**PAHEt** complex with 5:4 M:L stoichiometry, with all the N-H and O-H functions of the ligand deprotonated.

Single crystal analysis clearly shows the 12-MC-4 structure of the isolated compound (**1**). The compound crystallizes in triclinic singony, the space group *P-1*. The structure consists of 2D-coordination polymeric networks comprising from the dimeric anionic bis(12-MC-4) units **{[Cu$_5$(PAHEt-3H)$_4$(Ac)]$^{3-}$}$_2$** associated with eight sodium cations, two acetate anions and twelve water molecules taking part in sodium cations coordination, and solvate water molecules. The latter are linked with the polymeric networks with the help of H-bonds.

The pentanuclear 12-MC-4 units (Fig. 6) consist of five Cu(II) ions and four ligand residues doubly (N,O)-deprotonated by the hydroxamate group and monodeprotonated by the phosphonate function. Each ligand bridges three metal ions (one core and two ring ones). The coordination mode of the ligand can be described as $\{(N,O);(O',\mu_2-O'')\}$ bis(chelating)-and-bridging. Due to the realization of (N,O)-birding coordination of the hydroxamate group, a cyclic (-Cu-N-O-)$_4$ 12-MC-4 sequence forms a cavity arranged by four hydroxamate oxygen atoms and incorporating the fifth Cu(II) ion. The ligand residues are coordinated to two Cu(II) ions with the formation of two fused, five- and six-membered, chelate rings with a common C-N$_{(hydroxamate)}$ side. While the phosphonate group is involved in the six-membered ring, the hydroxamic oxygen atoms chelate another copper atom with the formation of the five-membered ring.
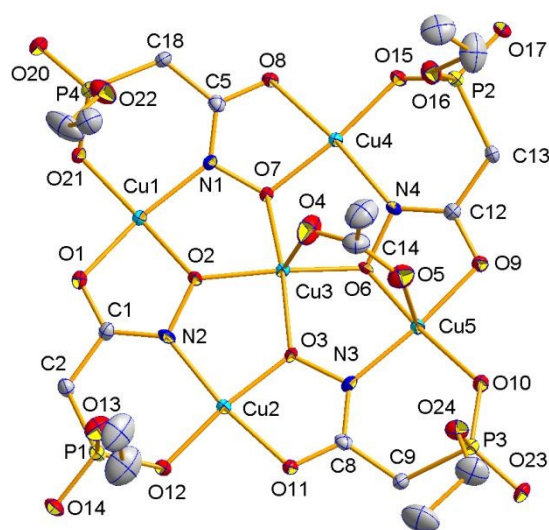

Fig. 6. The pentanuclear fragment of the structure **{Na$_4$(H$_2$O)$_6$(Ac)[Cu$_5$(PAHEt-3H)$_4$(Ac)]}$_2$·3H$_2$O** (**1**). Colour scheme: light blue = Cu, red = O, dark blue = N, gray = C, yellow = P.

The 12-MC-4 fragment indicates a ruffled conformation (Fig. 6). The ethoxy groups of phosphoester moieties are oriented on the same side of MC. The acetate ion coordinated in a (O,O')-bridging mode to the core (Cu(3)) and ring (Cu(5)) copper(II) ions is disposed on the same side. The deviations of MC from planarity are due to different, irregular conformations of the chelate and the bimetallic rings constituting the MC moiety. For example, the six-membered chelate rings involving

P(1) and P(2) atoms indicate nearly regular envelope conformation with the corresponding phosphorus atoms residing outside the chelate plane by 0.553(4) and 0.570(4) Å, respectively, while two other six-membered rings involving phosphorus indicate a distorted envelope conformation with C(9) and O(21) atoms being inclined from their chelate planes by 0.525(6) and 0.630(3) Å, respectively, by the opposite sides of the MC plane (that reside 1.57 A above and below the best least-squares plane of the MC core oxygens). While the four oxygen atoms and four ring Cu(II) ions define nearly ideal planes (the deviations of these atoms from their mean planes in each case do not exceed 0.017 Å), the declinations of the Cu atoms from the oxygen mean plane, and the oxygen atoms from the Cu mean plane, are significant and irregular. For example, the Cu(II) ions are situated out of the both sides of the oxygen mean plane, with the maximal declinations reaching 0.661(4) and 0.494(4) Å for the "top" and "bottom" sides, respectively. On the other hand, O(3) oxygen atom lies in fact in the tetracopper mean plane (with declination of only 0.014(3) Å), while O(2), O(6) and O(7) atoms are significantly declined from this plane (by 0.324(3), -0.578(3), and -0.309(3) Å, respectively). The dihedral angle between the core MC coppers and oxygens mean planes is 14.24(8)°. The Cu···Cu separations between the core (Cu(3)) and ring Cu(II) ions are in the range 3.1657(7)–3.3115(6) Å, and these between the ring metal atoms are in the range 4.5674(7)–4.6128(7) Å. The present geometrical parameters are similar to those seen in earlier studied hydroxamate 12-MC-4 structures.[43, 52]

Table 3. Selected bond lengths (Å) and angles (°) in the structure of **1**.

Cu1—O2	1.901 (3)	Cu3—O6	1.967 (2)
Cu1—O21^i	1.926 (3)	Cu3—O4	2.187 (3)
Cu1—O1	1.955 (3)	Cu4—O7	1.903 (2)
Cu1—N1	1.971 (3)	Cu4—O15	1.905 (2)
Cu1—O6^{ii}	2.439 (3)	Cu4—O8	1.929 (3)
Cu2—O3	1.864 (2)	Cu4—N4	1.961 (3)
Cu2—O12	1.900 (3)	Cu5—O9	1.942 (2)
Cu2—O11	1.947 (2)	Cu5—O6	1.949 (2)
Cu2—N2	1.970 (3)	Cu5—N3	1.952 (3)
Cu3—O3	1.893 (2)	Cu5—O10	1.961 (3)
Cu3—O7	1.916 (3)	Cu5—O5	2.338 (3)
Cu3—O2	1.926 (2)		
O2—Cu1—O21^i	170.84 (13)	O7—Cu4—O15	173.60 (11)
O2—Cu1—O1	80.75 (10)	O7—Cu4—O8	81.16 (10)
O21^i—Cu1—O1	95.23 (11)	O15—Cu4—O8	92.45 (11)
O2—Cu1—N1	90.00 (11)	O7—Cu4—N4	91.72 (11)
O21^i—Cu1—N1	93.44 (12)	O15—Cu4—N4	94.68 (11)
O1—Cu1—N1	170.17 (12)	O8—Cu4—N4	172.43 (11)
O2—Cu1—O6^{ii}	98.46 (11)	O9—Cu5—O6	81.70 (10)
O21^i—Cu1—O6^{ii}	89.92 (10)	O9—Cu5—N3	174.55 (12)
O1—Cu1—O6^{ii}	92.73 (10)	O6—Cu5—N3	93.14 (11)
N1—Cu1—O6^{ii}	91.91 (11)	O9—Cu5—O10	91.11 (11)
O3—Cu2—O12	172.95 (11)	O6—Cu5—O10	169.18 (11)

16

O3—Cu2—O11	81.62 (10)	N3—Cu5—O10	94.24 (12)
O12—Cu2—O11	91.38 (11)	O9—Cu5—O5	86.47 (11)
O3—Cu2—N2	89.90 (11)	O6—Cu5—O5	92.70 (11)
O12—Cu2—N2	97.11 (12)	N3—Cu5—O5	92.05 (12)
O11—Cu2—N2	171.40 (11)	O10—Cu5—O5	94.93 (12)
O3—Cu2—Na1	120.58 (8)		
O12—Cu2—Na1	52.43 (8)		
O11—Cu2—Na1	41.56 (7)		
N2—Cu2—Na1	146.87 (9)		
O3—Cu3—O7	164.08 (12)		
O3—Cu3—O2	87.70 (11)		
O7—Cu3—O2	89.54 (10)		
O3—Cu3—O6	92.04 (10)		
O7—Cu3—O6	86.94 (10)		
O2—Cu3—O6	166.18 (11)		

Symmetry transformations used to generate equivalent atoms: (i) *x*, *y*−1, *z*; (ii) −*x*, −*y*+1, −*z*+2

The Cu(II) ions in the MC find themselves in different geometric surroundings. The core Cu(3) ion is in a distorted square-bipyramidal surrounding of six oxygen atoms. The equatorial plane is formed by four hydroxmiato oxygen atoms, while the axial positions are occupied by the acetate oxygen and the hydroximate oxygen belonging to the neighbouring pentanuclear unit. The equatorial Cu-O bond lengths are in the range 1.894(3) - 1.968(3) Å.

Out of four ring metal ions, two (Cu(2) and Cu(4)) indicate a distorted square-planar geometry, while the other two (Cu(1) and Cu(5) a slightly distorted square-pyramidal geometry (τ_5 = 0.011 and 0.090, respectively). This difference is reflected in noticeably shorter equatorial Cu-O bond lengths in the case of tetracoordinated ions. The equatorial O_3N coordination of the ring metal ions is formed by three oxygen atoms (both of the hydroxamic group and one phosphonate) and the hydroxamate nitrogen atom. The Cu–O and Cu–N bond distances in the equatorial planes range from 1.863(3) to 1.955(3) Å, and from 1.863(3) to 1.955(3) Å, respectively, and are typical for Cu(II) 12-MC-4 complexes (Table 3). [43, 52-54]
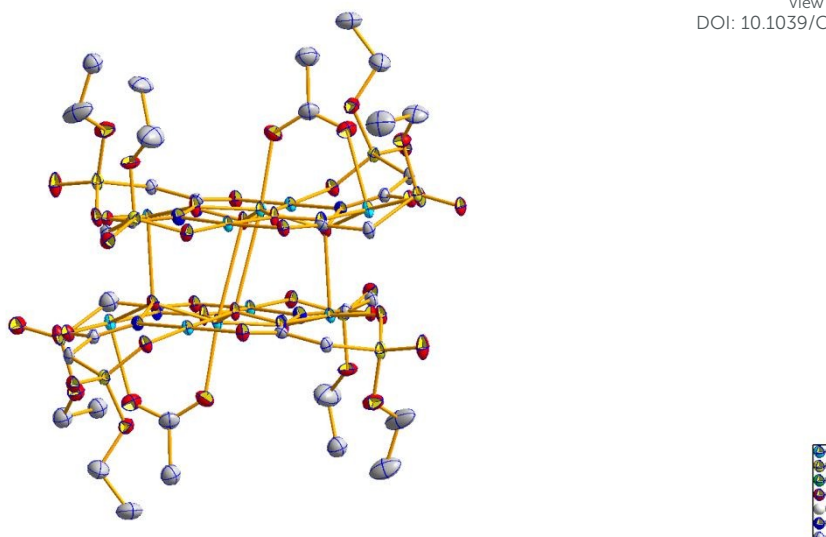
Fig. 7. Structure of $\{[Cu_5(PAHEt-3H)_4(Ac)]^{3-}\}_2$ complex anion in $\{Na_4(H_2O)_6(Ac)[Cu_5(PAHEt-3H)_4(Ac)]\}_2\cdot3H_2O$ (**1**). Colour scheme: light blue = Cu, red = O, dark blue = N, grey = C, yellow = P.

Two 12-MC-4 pentanuclear fragments are united into the double-decked centrosymmetric decanuclear complex anion (Fig. 7) on account of two pairs of elongated Jahn-Teller axial Cu···O contacts formed by Cu(II) ions with two hydroximic oxygen atoms of the neighbouring pentanuclear unit (Cu(1)···O(6)(-x, 1-y, 1-z) = 2.439(3) and Cu(3)···O(7))(-x, 1-y, 2-z) = 2.976(3) Å). These separations are substantially longer than the axial distance Cu(3)-O(4)(acetate) = 2.187(3). The shortest interdeck metal-metal separation Cu(2)···Cu(4)(-x, 1-y, 1-z) = 3.5078(7) Å.

Due to the presence of the exo-oriented phosphoryl and ethoxy moieties of the phosphoester groups, the 12-MC-4 units can act as ligands with respect to metal ions which in the present case gives rise to exo-coordination of sodium cations resulting in the formation of 2D-coordination polymeric motif. The four crystallographically independent sodium cations are bound to the decanuclear bis(metallacrown) moiety in different modes: (i) bidentatly via the C=O and P-O groups of two neighbouring ligands coordinated to the same ring Cu(II) ion (Na(1) and Na(4)) thus forming four-membered NaO_2Cu heterometallic rings, and (ii) monodentately via the phosphoryl group with simultaneous coordination to the axial acetate oxygen (Na(3)), thus forming NaO_2Cu ring with the same Cu(II) ion as well. At the same time, Na(2) did not form bond with MC being surrounded by five water molecules and the second, not bound to the MC, acetate ion (Fig. 8). Of note, Na(1) is also monodentately bound to the neighbouring decanuclear fragment via the phosphoryl group, thus uniting two bis(MC) moieties. The coordination of sodium cations is complemented to distorted octahedral (Na(2) and Na(4)) or pentacoordinated (Na(1) and Na(3)) by water molecules. The coordination polyhedra of eight sodium cations appear to share the edges with the neighbouring polyhedra thus forming a cluster $\{Na(1)Na(2)Na(4)Na(3)\}_2$ (Fig. 8) thus uniting four translational bis(12-MC-4) moieties into 2D layers spread parallel to bc plane of the crystal (Supplementary Fig. 5). The Na···Na separations in the octanuclear sodium clusters are in the range 3.323(2) – 3.611(2) Å. The translational

along *a* direction 2D layers are united into crystal due to numerous H-bonds and van der Waals interactions (Supplementary Fig. 6).
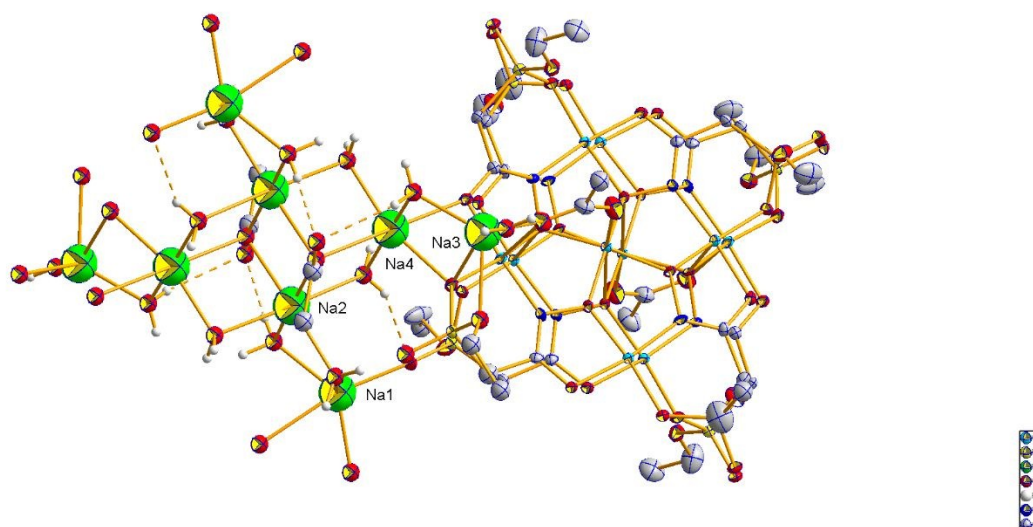
Fig. 8. Sodium cations coordination in the structure $\{Na_4(H_2O)_6(Ac)[Cu_5(PAHEt-3H)_4(Ac)]\}_2 \cdot 3H_2O$ (**1**). Colour scheme: light blue = Cu, red = O, dark blue = N, grey = C, yellow = P, green = Na. H-bonds are represented by dashed lines.

Stability of MCs under conditions of competitive complex formation as well as their reactivity with respect to strong chelating agents remains poorly studied. In this work, we attempted to establish the behaviour of the obtained 12-MC-4 species in reactions with bidentate chelating amines. In the case of reaction of 12-MC-4 with **dipy** (under **PAHEt** : **dipy** = 1:1 molar ratio) we found that the MC undergoes degradation, and as a result, 1D-coordination polymeric complex featuring mixed-ligand mononuclear units $\{[Cu(dipy)(PAHEt–2H)]\}_n \cdot 1.86nH_2O$ **(2)** is formed. Interestingly, the hydroxamic function is coordinated in (O,O')-chelating mode as evidenced by single crystal X-ray analysis of **(2)**.

The complex crystallizes in monoclinic singony, space group *P2₁/c*. The structure consists of infinite zigzag-like 1D-coordination polymeric chains formed by neutral mononuclear complex species **[Cu(dipy)(PAHEt–2H)]** and solvate water molecules associated with the chains (Fig. 9). The chains are spread along *b* directions of the crystal, the metal-metal separations between the neighbouring metal ions related by *P2₁* symmetry operation Cu(1)···Cu(1)(-x, 0.5+y, 0.5-z) = 6.9972(3) Å while the separation between the first and the third Cu(II) ions in the chain are equal to b parameter of the unit cell (12.0645(2) Å). A mononuclear unit consists of Cu(II) ion, neutral **dipy** ligands and a doubly deprotonated residue **PAHEt**. **dipy** ligands are coordinated in an usual mode with the formation of five-membered chelate rings. The hydroxamic ligand is coordinated in a $\{(O,O'),\mu\text{-}O\}$ chelating-and-bridging mode thus bridging two Cu(II) ions.
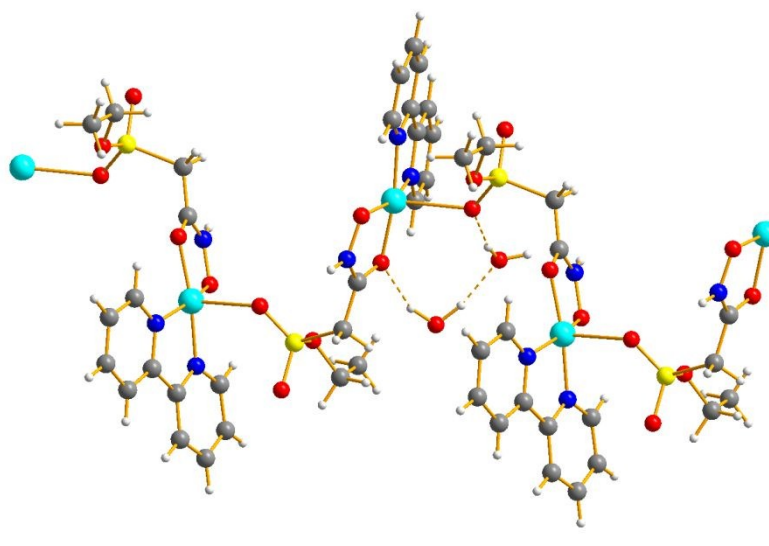
Fig. 9. Fragment of a polimeric chain of **{[Cu(dipy)(PAHEt–2H)]}$_n$·1.86nH$_2$O** (**2**) formed by the neutral mononuclear complex species **[Cu(dipy)(PAHEt–2H)]** and solvate water molecules associated with the chains. Colour scheme: light blue = Cu, red = O, dark blue = N, gray = C, yellow = P.

Cu(II) ion is situated in a distorted square-pyramidal surrounding (τ_5 = 0.141). The equatorial positions are occupied by two nitrogen atoms of **dipy** and two oxygen atoms of the hydroxamate group coordinated in a (O, O')- chelating mode. The Cu(1)-O(3) bond length with hydroximato oxygen atom (1.904(1) Å) is noticeably shorter than Cu(1)-O(2) and Cu-N (1.964(2) – 1.989(2) Å). The axial position is occupied by the oxygen atom of monodentately coordinated phosphonate group (Cu(1)-O(1) =2.416(1) Å), the axial bond length is significantly longer than the equatorial ones. The angular distortions of the coordination sphere are conditioned by the chelate formation (the bite angles O(2)-Cu(1)-O(3) and N(1)-Cu(1)-N(2) are decreased to 84.88(5) and 82.12(6)°, respectively) as well as by declination of the central atom from the least-square plane of four equatorial donor atoms by 0.2072(8)Å. The equatorial plane is also subjected to tetrahedral distortion: while both five-membered chelate rings are virtually planar (the maximal deviations of the atoms from their mean plane do not exceed 0.011(1) Å for the hydroxamate chelate and 0.025(1) Å for **dipy** chelate), the dihedral angle between their planes is 17.60(3)°.

Table 4. Selected bond lengths (Å) and angles (°) in the structure of **2**.

Cu1—O3	1.9040 (13)	O2—Cu1—N2	171.77 (6)
Cu1—O2	1.9627 (13)	O3—Cu1—N1	163.35 (6)
Cu1—N2	1.9813 (15)	O2—Cu1—N1	97.82 (6)
Cu1—N1	1.9891 (15)	N2—Cu1—N1	82.12 (6)
Cu1—O1	2.4159 (13)	O3—Cu1—O1	105.02 (5)
O3—Cu1—O2	84.88 (5)	O2—Cu1—O1	99.46 (5)
O3—Cu1—N2	92.87 (6)	N2—Cu1—O1	88.77 (5)
		N1—Cu1—O1	90.81 (5)

Conclusions

Solution and X-Ray studies on the Cu(II) complexes of ethylphosphonoacetohydroxamic acid (**PAHEt**) have demonstrated the first example of Cu(II) 12-MC-4 complex produced by the hydroxamic ligand, having an additional ethylphosphonate group in the β-position with respect to the hydroxamic group. Our results underline that the pH range of the formation of MC complexes and their overall stability depend on the peripheral chelating group with respect to the hydroxamate unit. When properly chosen, it can tune the thermodynamic properties of the MC assembly. Although the stability of the described MC complex is relatively low, **PAHEt** offers the formation of 12-MC-4 in a broad pH range. Optimization of ligands leading to the development of chelators forming MCs that have a high stability across a broad pH-range is in particular interest in the perspective of a potential use of MCs when a specific pH conditions are required, *i.e.* for selective binding of anions and cations. It worth noting that the binuclear species which could mimic **PAH** binding mode in inhibited enolase are not observed for **PAHEt**, neither in solution over all pH range studied nor in the solid state. This fact is not surprising as in the case of the enzyme active site the inhibitor binds to the metal ions already positioned in the protein matrix, thus having the majority of coordination sites being occupied. In the case of sodium cations, this results in realization of several alternative binding modes, both mono- and bidentate, which gives rise to two-dimensional coordination networks featuring decacopper-bis(12-MC-4) anionic modules and octanuclear sodium cationic clusters. One can expect that in the case of transition metal ions their exo-coordination can lead to discrete assemblies of high nuclearity as well as to the coordination polymers and MOFs with specific optical and magnetic properties. Moreover, the use of **PAH** ligand having -OH group instead of ethoxy function in **PAHEt** can result in the formation of more stable complexes with large negative charge (-6 in the case of Cu(II) 12-MC-4) due to the presence of an additional anionic group (with pK_a about 7). In its turn, this effect should be accompanied by a significant increase in ability of the formed MCs to bind extra metal ions in the plane of the metallamacrocylic scaffold. Such studies are underway in our laboratories.

Conflicts of interest

There are no conflicts to declare.

References

1.   B. Kurzak, H. Kozlowski and E. Farkas, *Coordination Chemistry Reviews*, 1992, **114**, 169-200.

2. R. Codd, *Coordination Chemistry Reviews*, 2008, **252**, 1387-1408.

3. M. Tegoni and M. Remelli, *Coordination Chemistry Reviews*, 2012, **256**, 289-315.

4. G. Mezei, C. M. Zaleski and V. L. Pecoraro, *Chemical Reviews*, 2007, **107**, 4933-5003.

5. P. Happ, C. Plenk and E. Rentschler, *Coordination Chemistry Reviews*, 2015, **289**, 238-260.

6. C. Y. Chow, H. Bolvin, V. E. Campbell, R. Guillot, J. W. Kampf, W. Wernsdorfer, F. Gendron, J. Autschbach, V. L. Pecoraro and T. Mallah, *Chemical Science*, 2015, **6**, 4148-4159.

7. M. Ostrowska, I. O. Fritsky, E. Gumienna-Kontecka and A. V. Pavlishchuk, *Coordination Chemistry Reviews*, 2016, **327**, 304-332.

8. C. Y. Chow, R. Guillot, E. Riviere, J. W. Kampft, T. Mallah and V. L. Pecoraro, *Inorganic Chemistry*, 2016, **55**, 10238-10247.

9. T. T. Boron, III, J. W. Kampf and V. L. Pecoraro, *Inorganic Chemistry*, 2010, **49**, 9104-9106.

10. J. T. Grant, J. Jankolovits and V. L. Pecoraro, *Inorganic Chemistry*, 2012, **51**, 8034-8041.

11. J. Jankolovits, C.-S. Lim, G. Mezei, J. W. Kampf and V. L. Pecoraro, *Inorganic Chemistry*, 2012, **51**, 4527-4538.

12. J. Jankolovits, J. W. Kampf, S. Maldonado and V. L. Pecoraro, *Chemistry-a European Journal*, 2010, **16**, 6786-6796.

13. C. Sgarlata, A. Giuffrida, E. R. Trivedi, V. L. Pecoraro and G. Areneite, *Inorganic Chemistry*, 2017, **56**, 4771-4774.

14. E. R. Trivedi, S. V. Eliseeva, J. Jankolovits, M. M. Olmstead, S. Petoud and V. L. Pecoraro, *Journal of the American Chemical Society*, 2014, **136**, 1526-1534.

15. J. Jankolovits, C. M. Andolina, J. W. Kampf, K. N. Raymond and V. L. Pecoraro, *Angewandte Chemie-International Edition*, 2011, **50**, 9660-9664.

16. C. Y. Chow, S. V. Eliseeva, E. R. Trivedi, T. N. Nguyen, J. W. Kampf, S. Petoud and V. L. Pecoraro, *Journal of the American Chemical Society*, 2016, **138**, 5100-5109.

17. E. Rajczak, V. L. Pecoraro and B. Juskowiak, *Metallomics*, 2017, **9**, 1735-1744.

18. I. Martinic, S. V. Eliseeva, T. N. Nguyen, F. Foucher, D. Gosset, F. Westall, V. L. Pecoraro and S. Petoud, *Chemical Science*, 2017, **8**, 6042-6050.

19. I. Martinic, S. V. Eliseeva, T. N. Nguyen, V. L. Pecoraro and S. Petoud, *Journal of the American Chemical Society*, 2017, **139**, 8388-8391.

20. L. Marchio, N. Marchetti, C. Atzeri, V. Borghesani, M. Remelli and M. Tegoni, *Dalton Transactions*, 2015, **44**, 3237-3250.

21. D. Bacco, V. Bertolasi, F. Dallavalle, L. Galliera, N. Marchetti, L. Marchio, M. Remelli and M. Tegoni, *Dalton Transactions*, 2011, **40**, 2491-2501.

22. E. Gumienna-Kontecka, I. A. Golenya, A. Szebesczyk, M. Haukka, R. Kraemer and I. O. Fritsky, *Inorganic Chemistry*, 2013, **52**, 7633-7644.

23. C. Atzeri, L. Marchiò, C. Y. Chow, J. W. Kampf, V. L. Pecoraro, M. Tegoni, *Chemistry – A European Journal*, 2016, **22**, 6482-6486.

24. A. V. Pavlishchuk, S. V. Kolotilov, M. Zeller, O. V. Shvets, I. O. Fritsky, S. E. Lofland, A. W. Addison and A. D. Hunter, *European Journal of Inorganic Chemistry*, 2011, 4826-4836.

25. A. V. Pavlishchuk, S. V. Kolotilov, M. Zeller, S. E. Lofland, M. A. Kiskin, N. N. Efimov, E. A. Ugolkova, V. V. Minin, V. M. Novotortsev and A. W. Addison, *European Journal of Inorganic Chemistry*, 2017, 4866-4878.

26. E. Gumienna-Kontecka, I. A. Golenya, N. M. Dudarenko, A. Dobosz, M. Haukka, I. O. Fritsky and J. Swiatek-Kozlowska, *New Journal of Chemistry*, 2007, **31**, 1798-1805.

27. J. Galezowska and E. Gumienna-Kontecka, *Coordination Chemistry Reviews*, 2012, **256**, 105-124.

28. K. P. Valery and H. R. Harry, *Aminophosphonic and aminophosphinic acids: Chemistry and Biological Activity*, John Wiley & Sons, LTD, New York, 2000.

29. The Brookhaven Protein Data Bank (http://www.rcsb.org) contains six entries with PAH (4ZA0, 2PTZ, 2PU0, 1L8P, 1EBG, 1ELS), and all of them are with enolase as inhibited enzyme.

30. *APEX2,* Bruker AXS Inc., Madison, Wisconsin, USA, 2007.

31. *SADABS*, Bruker AXS Inc., Madison, Wisconsin, USA, 2001.

32. G. M. Sheldrick, *Acta Crystallographica a-Foundation and Advances*, 2008, **64**, 112-122.

33. G. M. Sheldrick, *Acta Crystallographica a-Foundation and Advances*, 2015, **71**, 3-8.

34. M. Nardelli, *Journal of Applied Crystallography*, 1999, **32**, 563-571.

35. G. Gran, *Acta Chemica Scandinavica*, 1950, **4**, 559-577.

36. P. Gans, A. Sabatini and A. Vacca, *Journal of the Chemical Society-Dalton Transactions*, 1985, 1195-1200.
37. L. Alderighi, P. Gans, A. Ienco, D. Peters, A. Sabatini and A. Vacca, *Coordination Chemistry Reviews*, 1999, **184**, 311-318.
38. B. Kurzak, A. Kamecka, K. Kurzak, J. Jezierska and P. Kafarski, *Polyhedron*, 2000, **19**, 2083-2093.
39. T. Kiss, M. Jezowskabojczuk, H. Kozlowski, P. Kafarski and K. Antczak, *Journal of the Chemical Society-Dalton Transactions*, 1991, 2275-2279.
40. M. Pyrkosz, W. Goldeman and E. Gumienna-Kontecka, *Inorganica Chimica Acta*, 2012, **380**, 223-229.
41. F. Dallavalle and M. Tegoni, *Polyhedron*, 2001, **20**, 2697-2704.
42. E. Farkas, J. Szoke, T. Kiss, H. Kozlowski and W. Bal, *Journal of the Chemical Society-Dalton Transactions*, 1989, 2247-2251.
43. B. R. Gibney, D. P. Kessissoglou, J. W. Kampf and V. L. Pecoraro, *Inorganic Chemistry*, 1994, **33**, 4840-4849.
44. A. B. Lago, J. Pasan, L. Canadillas-Delgado, O. Fabelo, F. J. M. Casado, M. Julve, F. Lloret and C. Ruiz-Perez, *New Journal of Chemistry*, 2011, **35**, 1817-1822.
45. M. Tegoni, M. Remelli, D. Bacco, L. Marchio and F. Dallavalle, *Dalton Transactions*, 2008, 2693-2701.
46. M. Careri, F. Dallavalle, M. Tegoni and I. Zagnoni, *Journal of Inorganic Biochemistry*, 2003, **93**, 174-180.
47. M. Tegoni, F. Dallavalle, B. Belosi and M. Remelli, *Dalton Transactions*, 2004, 1329-1333.
48. M. Tegoni, L. Ferretti, F. Sansone, M. Remelli, V. Bertolasi and F. Dallavalle, *Chemistry-a European Journal*, 2007, **13**, 1300-1308.
49. D. Wyrzykowski, B. Pilarski, D. Jacewicz and L. Chmurzynski, *Journal of Thermal Analysis and Calorimetry*, 2013, **111**, 1829-1836.
50. D. Wyrzykowski, D. Zarzeczanska, D. Jacewicz and L. Chmurzynski, *Journal of Thermal Analysis and Calorimetry*, 2011, **105**, 1043-1047.
51. D. Wyrzykowski and L. Chmurzynski, *Journal of Thermal Analysis and Calorimetry*, 2010, **102**, 61-64.
52. Y. Song, J. C. Liu, Y. J. Liu, D. R. Zhu, J. Z. Zhuang and X. Z. You, *Inorganica Chimica Acta*, 2000, **305**, 135-142.
53. J. A. Halfen, J. J. Bodwin and V. L. Pecoraro, *Inorganic Chemistry*, 1998, **37**, 5416-5417.
54. J. Legendziewicz, M. Puchalska, Z. Ciunik and W. Wojciechowski, *Polyhedron*, 2007, **26**, 1331-1337.

Complex formation of copper(II), nickel(II) and zinc(II) with ethyl phosphonohydroxamic acid: solution speciation, synthesis and structural characterization

Table of contents entry

We present herein the thermodynamic and X-Ray characterisation of novel ethyl phosphonohydroxamic acid-based Cu(II) metallacrown, predominating in solution in a broad pH range.